https://ntrs.nasa.gov/search.jsp?R=19860015047 2020-03-20T15:40:34+00:00Z

N86-24518

1985

NASA/ASEE SUMMER FACULTY RESEARCH FELLOWSHIP PROGRAM

MARSHALL SPACE FLIGHT CENTER
THE UNIVERSITY OF ALABAMA

CALCULATIONS ON THE PRODUCTION AND USE OF SUPERFINE HOLOGRAPHIC X-RAY GRATINGS FOR ASTROPHYSICAL OBSERVATIONS

Prepared by:	Paul L. Csonka, Ph.D.
Academic Rank:	Professor
University and Department:	University of Oregon Institute of Theoretical Science
NASA/MSFC:	
Laboratory:	Space Science Laboratory
Division:	Astrophysics
Branch:	High Energy Physics
NASA Counterpart:	Martin C. Weisskopf
Date:	August 30, 1985
Contract No.:	NGT 01-008-021 The University of Alabama

CALCULATIONS ON THE PRODUCTION AND USE OF SUPERFINE HOLOGAPHIC X-RAY GRATINGS FOR ASTROPHYSICAL OBSERVATIONS

by

Paul L. Csonka
Professor of Physics
Institute of Theoretical Science
University of Oregon
Eugene, Oregon 97403

ABSTRACT

Superfine holographic x-ray gratings may be produced by transferring onto metal an inteference pattern generated by two branches of a sufficiently coherent x-ray beam, emitted in the form of synchrotron radiation from high energy electron storage rings. Generation of the coherent beam requires restrictions on the beam size. A calculation is presented which allows an exact evaluation of this restriction. The effect of defocusing optics on the expected resolution is also studied.

1. INTRODUCTION/OBJECTIVES

Superfine holographic x-ray gratings are to be produced by transferring onto metal an interference pattern generated by two branches of a sufficiently monochromatic and coherent x-ray beam[1]. Such an x-ray beam can be obtained by selecting an appropriately monochromatized and coherent portion of a synchrotron radiaton beam emitted by circulating electrons in a high energy electron storage ring, such as SSRL at Stanford.

Selection of the appropriate beam portion requires first of all adequate monochromatization. Denoting by λ the wavelength of the recording x-ray radiation, and by $\Delta\ell$ the maximum pathlength difference between the two branches of the imprinting beam, one has to have

$$\frac{\Delta\lambda}{\lambda} \lesssim \frac{1}{2} f_1 \frac{\lambda}{\Delta\ell} . \qquad (1)$$

Here f_1 is a constant between zero and unity, to be specified below. Second, the angular divergence, $\Delta\theta$, needs to be restricted as

$$\Delta\theta \lesssim f_2^{1/2} \left(\frac{\lambda}{\Delta\ell}\right)^{1/2} , \qquad (2)$$

where $0 \leq f_2 \leq 1$ is a constant. Third, the cross-section of the beam has to be limited to achieve adequate coherence, which, in turn requires that the effective size of the radiation source (here circulating electrons) be constrained depending on the size of the area over which the interference pattern is to be established. That, of course, will reduce the number of photons which can be used to produce interference, and increase the time which has to elapse while the pattern is imprinted on a photosensitive material (such as PMMA). It is, therefore, important to accurately evaluate the necessary beam size, to be able to restrict the source area as required, but no more. A calculation will be described here which enables one to evalute the necessary restriction in beam size under quite general conditions, as illustrated in Fig. 1. Superfine holographic x-ray gratings are expected to achieve line densities $\geq 10^5$ lines/mm. For an incident wavelength of λ = 100 Å at normal incidence on the grating, when the radiation is collected by an optical element with 1 arcsec accuracy, the intrinsic grating resolution is of the order of $\Delta\lambda/\lambda = 10^{-5}$. The question will be investigated to what extent this resolution can be approached in an actual instrument.

2. COHERENCE REQUIREMENTS

The notation is explained in Figs. 1 and 2. For any vector $\bar{v}$, we will write $|\bar{v}| = v$.

Referring to Fig. 2, one observes

$$L^2_{ik} = \left[-(\bar{L} + \bar{P}_{sk}) + \bar{P}_i\right]^2 \; ; \; i, k = 1, 2 \tag{1}$$

$$L_{ik} = \left\{(\bar{L} + \bar{P}_{sk})^2 - 2(\bar{L} + \bar{P}_{sk})\,\bar{P}_i + \bar{P}_i^{\,2}\right\}^{1/2}. \tag{2}$$

Introduce the notion

$$\bar{a}_k = \bar{L} + \bar{P}_{sk}, \tag{3}$$

and write a_{ky} and a_{kz} for the y and z component of $\bar{a}_k$. Since the coorindate axes are so chosen that the z component of P_1 and P_2 vanishes, one can rewrite (2) as

$$L_{ik} = \left\{a_{kz}^{\,2} + (a_{ky} - P_i)^2\right\}^{1/2}. \tag{4}$$

The

$$\Delta L_1 = L_{21} - L_{11} = |a_{1z}| \left\{\left[1 + \frac{(a_{1y} - P_2)^2}{a_{1z}^{\,2}}\right]^{1/2} - \left[1 + \frac{(a_{1y} - P_1)^2}{a_{1z}^{\,2}}\right]^{1/2}\right\} \tag{5}$$

$$\xrightarrow[|a_{1z}| \to \infty]{} \frac{(a_{1y} - P_2)^2 - (a_{1y} - P_1)^2}{2|a_{1z}|}.$$

Next we find the maximum value of ΔL_1. Clearly ΔL_1 will reach its highest value for any chosen point P_{s1},

when the point P_2 is such that for it L_{21}^2 is maximum, and at the same time P_1 is such that L_{11}^2 is minimum.

If P_{s1} is located in Region 1, then the minimum value of L_{11}^2 occurs for that P_1, for which $P_1 = a_{1y}$, and then $L_{11} = a_{1z}$. To find that P_2 for which L_{21}^2 is maximum, note that for the choice i = 2, Eq. (4) reaches extremum as a function of P_2, when

$$P_2 = -a_{1y} , \tag{6}$$

and this extremum is a minimum. Since L_{21}^2 is a second order polynomial in P_2, L_{21}^2 can have no other extremum. Its maximum value as a function P_2 is therefore reached at the endpoints of the allowed range of variation for P_2, i.e., at $P_2 = \pm D_y/2$. By direct inspection, the correct choice is

$$P_2 = - \frac{a_{1y}}{|a_{1y}|} \frac{D_y}{2} , \tag{7}$$

so that the maximum of L_{21}^2 is

$$L_{21}^2 = \left\{ a_1^2 + \left(|a_{1y}| + \frac{D_y}{2} \right) D_y \right\}^{1/2} , \tag{8}$$

and the maximum over P_1 and P_2 of ΔL_1, for a given P_{s1} is

$$\max \left[P_1, P_2 \right] \Delta L_1 = \left\{ a_{1z}^2 + a_{1y}^2 + \left(2|a_{1y}| + \frac{D_y}{2} \right) \frac{D_y}{2} \right\}^{1/2} - |a_{1z}|$$

$$\xrightarrow{|a_{1z}| \to \infty} \frac{1}{2|a_{1z}|} \left(|a_{1y}| + \frac{D_y}{2} \right)^2 . \tag{9}$$

Next, consider the case when P_{s1} is located in Region 2. We already know that L_{11} can have no extremum of any type in Region 2, nor can L_{21}. Therefore, that P_1 for which L_{11} is smallest, once P_{s1} is fixed, must lie on the boundaries of its allowed region of variation, i.e., at $\pm D_y/2$. Similarly, that P_2, for which L_{21} is maximum, must also lie there. By directly comparing the two possible choices, one finds

$$P_1 = (a_{1y}/|a_{1y}|)\, D_y/2$$

$$P_2 = -P_1 \qquad (10)$$

so that the maximum over P_1 and P_2 of ΔL_1 for a given P_{s1} is

$$\max [P_1, P_2]\Delta L_1 = \{a_{1z}^2 + (|a_{1y}| + \frac{D_y}{2})^2\}^{1/2}$$

$$-\{a_{1z}^2 + (|a_{1y}| - \frac{D_y}{2})^2\}^{1/2} \xrightarrow[|a_{1z}|\to\infty]{} \frac{1}{2|a_{1z}|}\, 4|a_{1y}|\, \frac{D_y}{2}\,. \qquad (11)$$

From Eqs. (9) and (11)

$$\max[P_1, P_2]\Delta L_1 \xrightarrow[|a_{1z}|\to\infty]{} \frac{1}{2|a_{1z}|}\begin{cases}(|a_{1y}| + \frac{1}{2} D_y)^2 & \text{in Reg. 1}\\ 2|a_{1y}|\, D_y & \text{in Reg. 2}\end{cases}$$

$$= \frac{1}{2|a_{1z}|}\, f_y^{\,2} \qquad (12)$$

where f^2 is defined by the above.

The maximum of ΔL_{11} over all possible P_1, P_2 and P_{s1} can now be easily evaluated. Denoting the maximum value of $|a_{1y}|$ by $|a_{1y}|_{max}$, one finds

$$\max[P_1, P_2, P_{s1}]\Delta L_{11} \xrightarrow[|a_{1z}|\to\infty]{} \frac{1}{2|a_{1z}|}\begin{cases}(|a_{1y}|_{max} + \frac{1}{2} D_y)^2 ; \text{in Reg. 1}\\ 2|a_{1y}|_{max}\, D_y \quad ; \text{in Reg. 2}\end{cases} \qquad (13)$$

So far we dealt with the source and interference planes as if they were one dimensional. The second surface dimension, along the x axis, can be easily incorporated, by allowing $\bar{P}_i$ and $\bar{a}_k$ to have x components. Then by similar reasoning

$$\max[\bar{P}_1, \bar{P}_2]\Delta L_1 = \{a_{1z}^2 + \sum_{n=x,y} (|a_{1n}| + \frac{1}{2} D_n)^2\}^{1/2} -$$

$$-\{a_{1z}^2 + \sum_{n=z,y} (|a_{1n}| - \frac{1}{2} D_n)^2\}^{1/2} \qquad (14)$$

$$\xrightarrow[|a_{1z}|\to\infty]{} \frac{1}{2|a_{1z}|} \sum_{n=x,y} f_n^2$$

and the definition of f_x is obtained from that of f_y by changing all subscripts y to x.

In the special case when $\bar{L}$ is parallel to z and both the source plane and the interference plane are perpendicular to L, then Eq. (13) reduces to the known formula

$$\max[P_1, P_2]\Delta L_{11} \xrightarrow[|a_{1z}|\to\infty]{} \frac{1}{2|a_{1z}|} \begin{cases} \frac{1}{4}(|D_s| + |D|)^2 ; \text{ if } D_s \leq D \\ |D_s|\,|D_y| \quad ; \text{ if } D_s > D \end{cases} \qquad (14a)$$

and f_n^2 goes over into the known[1] function Δ_n^2.

III. DEFOCUSING ELEMENTS

Assume that the colletor has an intrinsic angular inaccuracy of ε. For AXAF ε is of the order of 2×10^{-5} radians. It will also be assumed that the detector size can be made arbitrarily small, so that the instrument resolution is not limited by detector size. For AXAF, that assumption is not automatically valid, but for superfine holographic x-ray gratings, in many cases, instrument resolution is limited by the location of the grating, and that is the topic to be studied here.

The geometry and notation is explained in Fig. 3. The angular deviation introduced by the grating will be detectable over the "noise" caused by finite ε and ℓ, if

$$\tan \psi \gtrsim \frac{F}{L} \tan \varepsilon + \frac{\ell}{L} \tan \theta \ . \tag{15}$$

The deviation in the detector plane induced by the grating in m^{th} order near normal incidence for wavelength λ will differ from that for $\lambda + \Delta\lambda$ by

$$L\Delta\lambda \frac{d\tan\psi}{d\cos\psi} \frac{d\cos\psi}{d\lambda} = \Delta\lambda L \frac{\pm m}{d} \frac{d\tan\psi}{d\cos\psi} = \frac{\Delta\lambda}{\lambda} Lf(\psi) \tag{16}$$

where f is defined as

$$f(\psi) = -(\cos^2\psi - \tan^2\psi)/\sin\psi \ .$$

Therefore, the image of a single point source in m^{th} order, near normal incidence, formed by two different wavelengths, λ and $\lambda + \Delta\lambda$, will be distinguishable, provided that

$$\frac{\Delta\lambda}{\lambda} \gtrsim \frac{F}{L} \frac{\tan \varepsilon}{f(\psi)} + \frac{\ell}{L} \frac{\tan \theta}{f(\psi)} \ . \tag{17}$$

For AXAF, one has $F = 10^3$ cm, $\varepsilon \simeq 2 \times 10^{-5}$ radians, and $\theta = 0.1$. Then

$$\frac{\Delta\lambda}{\lambda} \gtrsim \left[\frac{2 \times 10^{-2}}{L} + \frac{\ell}{L} 0.1003\right] \frac{1}{f(\psi)} \ , \tag{18}$$

if L and ℓ are measured in centimeters. Now clearly the best choice is $\ell = 0$, and then

$$\frac{\Delta\lambda}{\lambda} \gtrsim \frac{2 \times 10^{-2}}{L \text{ (in cm)}} \quad \frac{1}{f(\psi)} \; . \tag{19}$$

For superfine gratings with $d = 10^{-6}$ cm, and $\lambda = 100$ Å, one has $f(\psi) = 1/\sqrt{2}$, and

$$\frac{\Delta\lambda}{\lambda} \gtrsim \frac{1.41 \times 10^{-2}}{L \text{ (in cm)}} \; ; \text{ for } \lambda = 100 \text{ Å} \; . \tag{20}$$

For gratings with diameter $\lesssim 20$ cm in AXAF, one has $L \lesssim 100$ cm, which would give $\Delta\lambda/\lambda \gtrsim 1.4 \times 10^{-4}$ for $\lambda = 100$ Å. This resolution is clearly far from the intrinsic resolution of the grating, which is about 5×10^{-6} for this wavelength.

To increase the instrument resolution, one can either increase the grating diameter, D_g, or increase L.

The increase in resolution with D_g is linear, and we will not concern ourselves further with that variation.

To increase the resolution while keeping D_g fixed, one may introduce a defocusing element at a distance ℓ_d before the original focal plane. If that element changes θ by a factor h^{-1} $(h > 1)$, then the new focal plane will be farther from the defocusing element than the original focal plane was, by a factor h. Then the wavelength resolution of the new instrument will be given by Eq. (17), provided that in it one substitutes for F, L, ℓ, and θ the new effective values: F', L', ℓ', and θ'. Assuming $F, L > \ell_g > \ell$, one has

$$F' = (F - \ell_g) + h\ell_g = F + \ell_g (h - 1)$$

$$L' = L + \ell_g (h - 1)$$

$$\ell' = h\,\ell$$

$$\theta = h^{-1}\,\theta$$

and the new resolution is

$$\frac{\Delta'\lambda}{\lambda} \geq \frac{F+\ell_g(h-1)}{L+\ell_g(h-1)} \frac{\tan \varepsilon}{f(\psi)} + \frac{h\ell}{L+\ell_g(h-1)} \frac{\tan (h^{-1}\theta)}{f(\psi)} . \qquad (21)$$

When $\ell = 0$, and the defocusing element is located close behind the grating, $\ell_g \approx L$, then

$$\frac{\Delta'\lambda}{\lambda} \geq \frac{1}{h} \frac{F}{L} \left(1 + \frac{h-1}{F/L}\right) \frac{\tan \varepsilon}{f(\psi)} . \qquad (22)$$

Clearly, for F/L large, the resolution will improve essentially linearly with h, up to values $h \approx F/L$. Beyond that, the resolution tapers off, and approaches its asymptotic value for large h:

$$\frac{\Delta'\lambda}{\lambda} \xrightarrow[h\to\infty]{} \frac{\tan \varepsilon}{f(\psi)} ,$$

which is, of course, the intrinsic resolution of the grating.

For AXAF, it appears possible to reflect the beam at least once, maybe twice (once backward and once forward) along the axis of the focusing telescope. In that way one could increase the wavelength resolution for $F - L = 900$ cm, $h = 21$, to 66% of its intrinsic value; i.e., to $\Delta\lambda/\lambda = 7.3 \times 10^{-6}$ at $\lambda = 100$ Å. Reflecting the beam in this manner causes no difficulty in this wavelength range, since the reflectivity of multilayer mirrors can approach 66%. However, the use of multilayer reflection optics will reduce the bandwidth of the instrument.

An alternative option would be to place the same instrument into Spacelab. Defocusing could be done with grazing incidence mirrors, which would alleviate the problem of wavelength reduction. Additional reflections would not be required if the dimensions of Spacelab are to be as envisioned today.

ACKNOWLEDGEMENTS

I wish to thank Mike Hettrick of BNL and Martin Weisskopf of MSFC for interesting discussions on this topic.

REFERENCES

1. Csonka, Paul L., "Holographic X-Ray Gratings Generated by Synchrotron Radiation", J. Appl. Phys., 52, 2692 (1981).

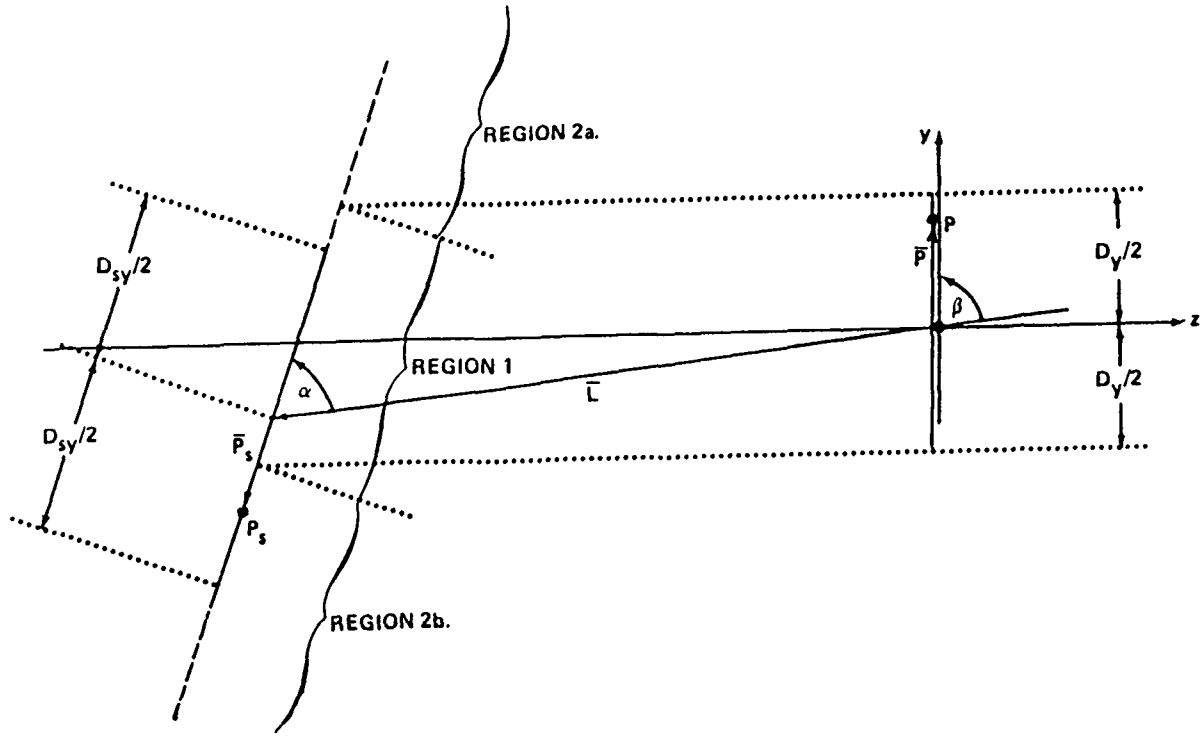

Figure 1. The interference pattern is generated on the "interference surface." It has diameter (in the y,z plane) D_y. The point P lies on this surface. The source of the beam is a plane whose diameter (in the y,z plane) is D_{sy}. The point P_s lies in the source plane. The center of the beam is along the vector $\bar{L}$, and the radius vector of P and P_s is $\bar{P}$ and $(\bar{L} + \bar{P}_s)$, respectively. The plane in which the interference takes place is divided into three regions: Regions 1, 2a, and 2b, which together cover the whole plane. Region 1 is defined as the projection along y onto this plane of the area on which the interference pattern is generated. There are no restrictions on the orientation of the source plane and that of the interference plane with respect to $\bar{L}$.

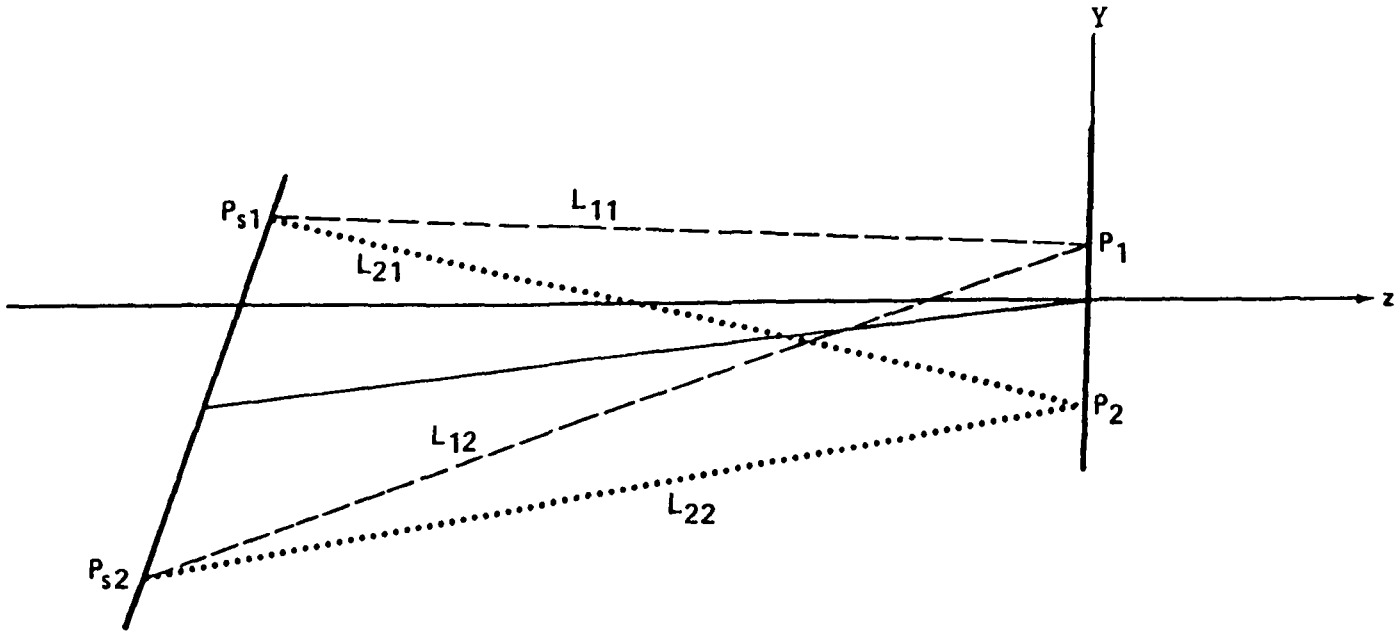

Figure 2. The optical pathlength to P_1 from P_{s1} and P_{s2} is L_{11} and L_{12}, respectively. The optical pathlength to P_2 from P_{s1} and P_{s2} is L_{21} and L_{22}, respectively. The optical path difference $\Delta L_i = (L_{2i} - L_{1i})$ measures the extent to which the interference plane deviates from a wavefront for a wave emitted at P_{si}.

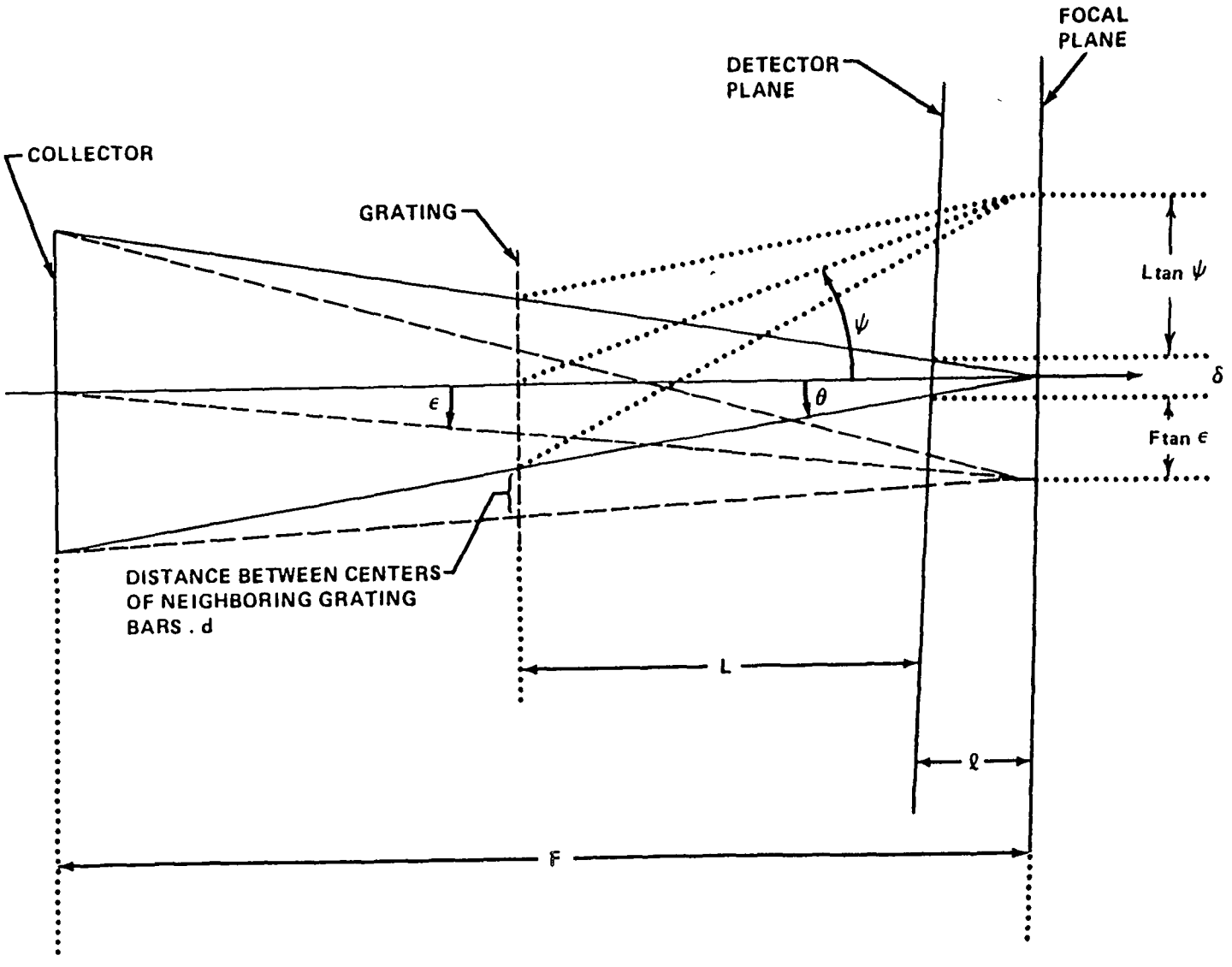

Figure 3. The collector has focal length F, and focuses radiation with an angular divergence θ in the focal plane, with an angular inaccuracy ε. As a result of this inaccuracy, the position of the image on the focal plane is undetermined to within a distance F tan ε. The size at the detector plane of an image focused on a point at the focal plane is $\delta = \ell \tan \theta$. The grating introduces an angular deviation ψ, causing the image point in the focal plane to be displaced by a distance L tan ψ. This displacement will be detectable if L tan ψ F tan ε + ℓ tan θ.